



This is a repository copy of *Comparison of peak armature and peak field winding currents for different topologies of 10 MW superconducting generators under short-circuit conditions*.

White Rose Research Online URL for this paper:
<http://eprints.whiterose.ac.uk/106746/>

Version: Accepted Version

Article:

Santos, F.V., Guan, Y., Azar, Z. et al. (4 more authors) (2016) Comparison of peak armature and peak field winding currents for different topologies of 10 MW superconducting generators under short-circuit conditions. *IEEE Transactions on Applied Superconductivity*, 26 (8). 5208407. ISSN 1558-2515

<https://doi.org/10.1109/TASC.2016.2615077>

© 2016 IEEE. Personal use of this material is permitted. Permission from IEEE must be obtained for all other users, including reprinting/ republishing this material for advertising or promotional purposes, creating new collective works for resale or redistribution to servers or lists, or reuse of any copyrighted components of this work in other works.

Reuse

Unless indicated otherwise, fulltext items are protected by copyright with all rights reserved. The copyright exception in section 29 of the Copyright, Designs and Patents Act 1988 allows the making of a single copy solely for the purpose of non-commercial research or private study within the limits of fair dealing. The publisher or other rights-holder may allow further reproduction and re-use of this version - refer to the White Rose Research Online record for this item. Where records identify the publisher as the copyright holder, users can verify any specific terms of use on the publisher's website.

Takedown

If you consider content in White Rose Research Online to be in breach of UK law, please notify us by emailing eprints@whiterose.ac.uk including the URL of the record and the reason for the withdrawal request.



eprints@whiterose.ac.uk
<https://eprints.whiterose.ac.uk/>

Comparison of Peak Armature and Field Winding Currents for Different Topologies of 10 MW Superconducting Generators under Short-Circuit Conditions

F. Vedeño-Santos, Y. Guan, Z. Azar, *Senior Member, IEEE*, A.S. Thomas, G.J. Li *Member, IEEE*, M. Odavic, *Member, IEEE*, Z.Q. Zhu, *Fellow, IEEE*

Abstract – This paper studies the peak armature and peak field winding currents for three different topologies of 10 MW partial High Temperature Superconducting Generators (HTSGs) under Short-Circuit Conditions (SCC) by simulation. The investigated partial HTSGs employ copper armature windings and superconducting field windings with different armature and rotor topologies, i.e. iron cored armature and rotor, air cored armature and rotor, and iron cored armature and air cored rotor. For each HTSG topology, the investigation includes: (i) the field winding current control strategies, (ii) the influence of operating field current, and (iii) the ratings of circuit breakers for limiting the peak armature and peak field winding currents. The results can provide guidelines for determining the peak armature and peak field currents of HTSGs and also the possibility of limiting them by employing circuit breakers under SCC.

Index Terms – air-cored, fault conditions, iron-cored, short-circuit, superconducting machines

I. INTRODUCTION

Wind power generation is one of the fast growing renewable technologies. In order to meet the increasing energy demand and reduce the cost of energy, wind turbines with higher power ratings are needed. For off-shore wind turbines, power ratings of 10 MW and above are being considered as the most promising for the near future. This is due to the fact that the foundation cost, which is the most predominant, increases slower than the cost of the power rating [1]. As a consequence of high power ratings, large scale direct drive generators with conventional topologies become large and heavy. This increases the difficulties for their installation and

transportation, leading to increased total cost of energy output of wind turbines.

Superconducting Generators (SGs) have the potential of providing high power with smaller size and weight than conventional generator technologies [2]. The most predominant High Temperature Superconducting Generator (HTSG) is the partial SG, i.e. copper armature windings and superconducting field windings, [3]. The three studied topologies for partial HTSG are:

- (i) Both iron cored armature and rotor (designated as “Iron cored”).
- (ii) Iron cored armature and air cored rotor (designated as “Mixed cored”).
- (iii) Both air cored armature and rotor (designated as “Air cored”).

Furthermore, in addition to the above aforementioned topologies there is an air cored armature and iron cored rotor topology which was discarded after considering its advantages and disadvantages due to weight and economic reasons.

However, regardless of the chosen topology, the HTS winding is the most expensive component of the generator, and hence, has to be protected against electrical faults [4]. A three-phase short-circuit is one of the most critical faults which may happen in an electrical machine. When a three-phase short-circuit occurs armature current increases together with field winding current in order to satisfy the principle of constant flux linkage [5].

It is therefore mandatory to make sure that the mechanical design of the SG is able to withstand the mechanical stress due to short-circuit currents and to set the values for protection of the system. Furthermore, the increase of field winding current due to three-phase short-circuit might result in catastrophic consequences since the state of superconductivity of a HTS material is limited by its critical temperature, current density and magnetic field [6]. Hence, it is necessary to take into account the maximum values of the armature and field winding currents for the electromagnetic design of the HTSG.

Many researchers have recently focused on the design of SGs [7]-[15]. However, three-phase Short-Circuit Conditions (SCC) are not taken into account during the electromagnetic design stage. Literatures that deal with SGs under fault conditions are limited [4], [16]-[18]. In [16] a series of simulations are carried out to study the loss of superconductivity of a field coil in a 100 MVA SG under fault conditions that can cause the quench in HTS materials in terms of (i) current, (ii) temperature and (iii) magnetic

The work is financially supported by the European Union’s Seventh Framework Programme for research, technological development and demonstration under grant agreement No. 308974, Project name: Innovative Wind Conversion Systems (10-20MW) For Offshore Applications (INNWIND).

F. Vedeño-Santos was with the University of Sheffield and is now with the School of Engineering & Built Environment, Edinburgh Napier University, Edinburgh EH10 5DT, UK (e-mail: f.vedrenosantos@napier.ac.uk).

Y. Guan, G.J. Li, M. Odavic, and Z.Q. Zhu are with the Department of Electronic and Electrical Engineering, University of Sheffield, Sheffield, S1 3JD, U.K. (e-mail: y.guan@sheffield.ac.uk; m.odavic@sheffield.ac.uk; g.li@sheffield.ac.uk; z.q.zhu@sheffield.ac.uk).

Z. Azar and A.S. Thomas are with Siemens Wind Power, Sheffield, S3 7HQ, U.K. (e-mail: ziad.azar@siemens.com; arwyn.thomas@siemens.com).

field [2]. Quench is most likely to occur when the operating current of the field winding exceeds the critical current of the HTS material. It is also stated that if the transient short-circuit field current slightly exceeds the critical value, the thermal quench (high increase of the temperature in the field winding coil) does not appear and the coil is able to return to its superconducting state. However, when the transient short-circuit field current exceeds its critical current by more than 18%, the field winding is unable to return to the superconducting state since the thermal quench appears and the cooling system is unable to keep the temperature low enough. Furthermore, when a fault occurs the magnetic field at the field winding coil exceeds its critical value [16]. However, a more recent theoretical study presented in [17] proves that the magnetic field does not exceed the critical value under fault conditions since the maximum magnetic field in the field winding coil occurs when it operates under no-load conditions, whereas the lowest value occurs when the system is under fault conditions.

In [4], the experimental study of a 100 kW HTSG with an iron cored armature and air cored rotor under three-phase short-circuit conditions is presented. It is concluded that if the fault is cleared in a short time after the occurrence of short-circuit the temperature of the superconducting field winding will not be affected. Furthermore, the control is unable to prevent the peak armature and peak field winding currents from exceeding their critical values. It is also worth noticing that the peak field winding current has a linear dependency with the operating field winding current. A similar study has been carried out in [18] for a 100 kW HTSG with both iron cored armature and field rotor. Authors in [18] have shown that the peak field winding depends linearly on the operating field winding current, similar to the findings in [4]. However, contrary to [16] a sudden increase in the field winding current (higher than 18% of its critical value) does not produce thermal quench since the SG is able to go back to normal operation. Regarding the peak armature current, it has been increased by 3 times for a HTSG with an iron cored armature and an air cored rotor [4] and 6 times for a HTSG with both iron cored armature and rotor [18] under three phase SCC.

The aim of this paper is to provide some guidelines to determine the peak armature and peak field currents of HTSGs under SCC. Moreover, the influence of the field winding control on the armature and field currents is investigated on three different 10 MW HTSGs for wind turbines. The paper is organized as follows. In section II, the topology of each investigated HTSG as well as the electrical model for the SCC are described. In section III, the influence of the field winding control is studied for each SG. In section IV, the influence of the operating field current on both peak armature and peak field currents is investigated. In section V, the influence of the clearing time of circuit breakers for the short circuit is researched. Finally, section VI is the conclusions.

II. HTSG AND SHORT-CIRCUIT MODELS

A. HTSG Topologies

In order to have a fair comparison, the three major partial HTSGs investigated are designed for the same specifications: rated power, line-to-line voltage, frequency, slots and pole number and speed.

The HTSGs are optimized for the same stator copper loss, 495 kW, considering the end winding losses. The field winding is designed with the second generation HTS material YBCO. The operating temperature of the HTS material is assumed to be 30 K. The critical current of the HTS material is shown in Fig. 1. The current density of SC coil has a 17.3% of safety margin in respect to maximum load the HTSGs can endure for the Iron cored topology whereas for the Mixed and Air cored topologies the safety margin is 17.4%. For each HTSG, the stator yoke thickness, stator slot height and width, and rotor pole width/SC coil pitch are globally optimized to achieve the target power, 10 MW, with the shortest stack length.

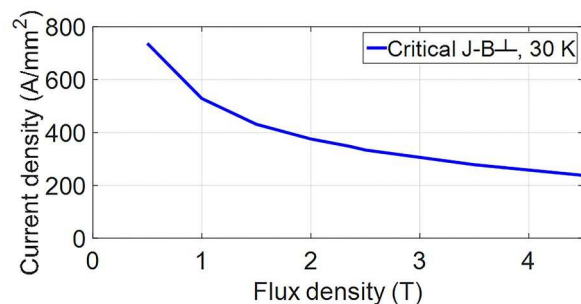


Fig. 1 Critical current density vs. flux density of the SC material (2G HTS YBCO).

The design of the HTSG finishes by adding the screens. Screens are usually constructed by drawing upon empirical knowledge since the effective mechanisms for their design are relatively complicated and diverse [19]. As a consequence, the screens are initially designed but not optimized for each HTSG. The cross section for the Iron, Mixed and Air cored HTSG shown in Fig. 2 (a), (b) and (c), respectively.

The electrical model of HTSGs, in dq frame, is shown in Fig. 3 [20], where R_s is the stator resistance per phase, L_l is the stator leakage inductance, L_{md} and L_{mq} are the d-axis and q-axis magnetizing inductances viewed from the stator, R'_{kd} , R'_{kq1} and R'_{kq2} are the d-axis resistance and q-axis resistances of the screen referred to the stator respectively. L'_{kd} , L'_{kq1} and L'_{kq2} are the d-axis and q-axis leakage inductances of the screen referred to the stator respectively. The rotor of the SG is defined by the R'_f and L'_{lfd} which are the resistance and leakage inductance of the rotor both referred to the stator. Finally, V_x , ϕ_x , i_x , i_{fx} , and i_{kx} represent the voltage, flux, stator current, field current, screen current and, $x = d$ or q for d- or q-axis. Finally, ω_r represents the angular frequency. Further details and equations for the electrical model can be found in [20].

The design of the HTSG and the calculation of its parameters is done by using the finite element software MAXWELL. A summary of the mechanical and electrical parameters of each studied HTSG are given in Table I.

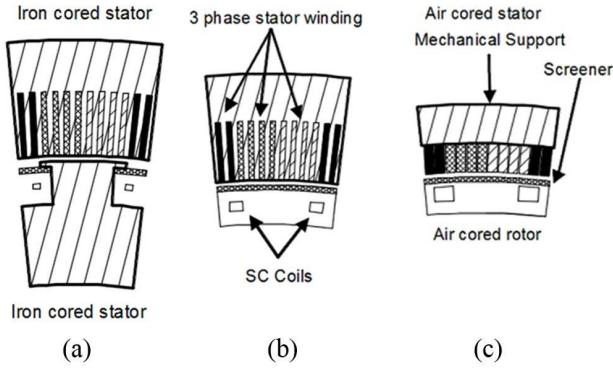


Fig. 2 Cross sections of (a) Iron, (b) Mixed and (c) Air cored HTSGs.

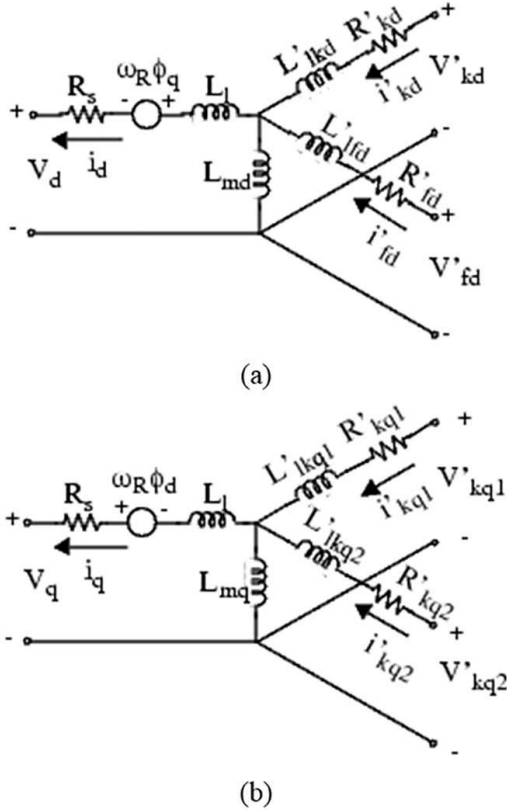


Fig. 3 Synchronous machine model. (a) d-axis, (b) q-axis [20].

TABLE I FEATURES OF 10 MW HTSG

| Parameter | Iron Cored | Mixed Cored | Air Cored | |
|--|------------|-------------|-----------|-----|
| Power (MW) | | 10 | | |
| Line-to-line voltage (V) | | 3300 | | |
| Frequency (Hz) | | 2.56 | | |
| Slots | | 384 | | |
| Pole number | | 32 | | |
| Speed (r.p.m) | | 9.6 | | |
| Stator diameter (m) | | 7 | | |
| Superconducting material | | 2G HTS YBCO | | |
| Axial length (m) | 1.2 | 1.06 | 0.95 | |
| Rotor outer diameter (m) | 3.0443 | 3.0513 | 3.225.5 | |
| Dimensions of SC coil (mm) | 7.9×12.65 | 30.6×49 | 43.3×69.3 | |
| Dimensions of SC wire (mm) | | 9.99×0.225 | | |
| Length of SC wire (km) | 5.35 | 81.66 | 156.40 | |
| Area of SC coil per pole (mm ²) | 200 | 3000 | 6000 | |
| SC coil current density J _{sc} (A/mm ²) | 345 | 217 | 194 | |
| Number of turns per SC coil | 89 | 1335 | 2669 | |
| Weight of iron (t) | 136.3 | 64.6 | 29.2 | |
| Rated field current (A) | 753 | 492 | 432 | |
| Stator | Core type | Iron | Iron | Air |

| | | | | |
|--------------|------------------------------|--------|--------|--------|
| | R_s (pu) | 0.0302 | 0.0638 | 0.0732 |
| | L_l (pu) | 0.0129 | 0.0047 | 0.0376 |
| | L_{md} (pu) | 0.0160 | 0.0043 | 0.0463 |
| | L_{mq} (pu) | 0.0182 | 0.0154 | 0.0058 |
| | R_{kd} (pu) | 0.0217 | 0.0217 | 0.0217 |
| | L_{lkd} (pu) | 0.0008 | 0.0008 | 0.0008 |
| | R_{kq1} (pu) | 0.0108 | 0.0108 | 0.0108 |
| | L_{lkq1} (pu) | 0.0004 | 0.0004 | 0.0004 |
| | R_{kq2} (pu) | 0.0108 | 0.0108 | 0.0108 |
| | L_{lkq2} (pu) | 0.0004 | 0.0004 | 0.0004 |
| Field | Core type | Iron | Air | Air |
| | R_{fd} (pu) | 0.0001 | 0.0001 | 0.0001 |
| | L_{ffd} (pu) | 0.0115 | 0.0099 | 0.0074 |

B. Short-Circuit Model

The HTSG is modelled in MATLAB Simulink software, according to the model described, Fig. 3. The armature windings are fed by a balanced three phase AC voltages, whereas the field winding is fed through a controllable DC voltage source, as shown in Fig. 4. The field winding lacks of a dump resistor since it might not be necessary in real applications [4] and its influence is inexistent on the peak field current [18]. The three armature phase SCC can be simulated at a specific time by turning on the two switches, S1 and S2.

Some assumptions regarding the SCC have to be made. Before short-circuit arises the HTSG operates at the rated conditions. The rotor speed is assumed to be constant and fixed at the rated speed before and after the SCC to simplify the modelling, although in real case the speed varies with time. This assumption is reasonable because the change in the speed is not only related to the HTSG but also with the speed-governing system and the inertia of the system, which is quite large for direct-drive wind turbines. The AC voltage system is also assumed to be an infinite power source.

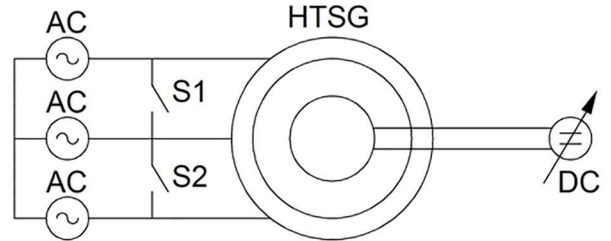


Fig. 4 Electrical scheme for SCC.

III. INFLUENCE OF FIELD WINDING CONTROL STRATEGY ON PEAK ARMATURE AND PEAK FIELD CURRENTS UNDER SCC

In this section the influence of the field winding control is investigated for the three different HTSGs. A three-phase short circuit is simulated starting at 4.5 seconds when the HTSG is operated at the rated conditions. The short circuit lasts for 5.5 seconds, in order to see the effect of three different field winding control strategies on the armature and field winding currents for the three HTSGs. The first control strategy (Control 1) keeps the field winding voltage constant while the short circuit occurs (Fig. 5, blue squares). The second control strategy (Control 2) reduces the field winding voltage to zero during the short circuit (Fig. 5, red crosses). The third control strategy (Control 3) reverses the field winding voltage under SCC (Fig. 5, black diamonds).

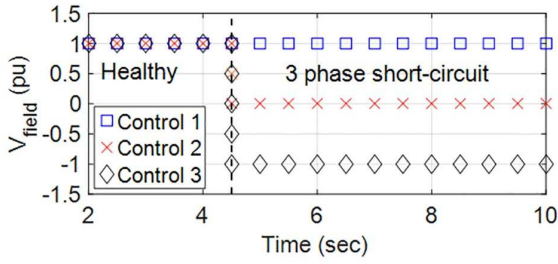


Fig. 5 Field voltage applied to the field winding variation when three phase short circuit occurs.

The use of the first and second control strategies does not involve any increase in the cost of field winding converter, since there are no changes in the supplied voltage for the first control strategy whilst for the second control strategy it can be achieved by simply making a short-circuit in the terminals of the field winding. However, for the case of the third control strategy, the cost of field winding converter increases since it is necessary to provide the field converter with the capability of reversing the voltage.

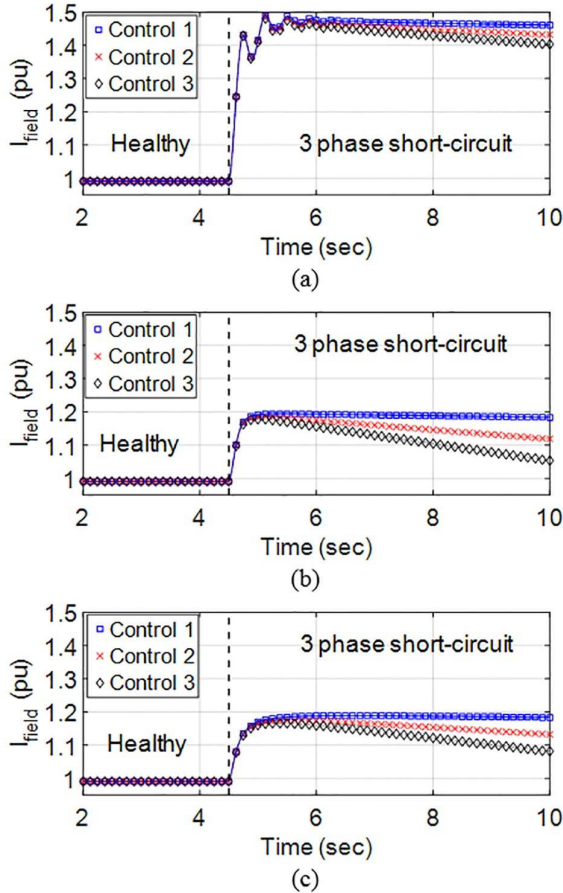


Fig. 6 Field current variation when three phase short circuit occurs. (a) Iron cored, (b) Mixed cored, and (c) Air cored HTSG.

The variations of field winding current and armature current under SCC are shown in Fig. 6, Fig. 7, and summarized in Table II. It is found that there is negligible influence of control strategies on the peak armature current for all three HTSGs. However, for the iron cored HTSG, the control strategy 3 can reduce the peak field current by 0.47% compared to control strategy 1, Fig. 6 (a). For the mixed and air cored HTSGs, the reduction is 1.33%, Fig. 6 (b) and Fig. 6 (c). However, the influence of the winding

field control on the peak armature and field winding currents is generally negligible.

For a wind turbine the fault ride through capabilities are often necessary. This can be achieved by applying the control strategy 3, which might reduce the field winding current to acceptable values for the mixed and air cored HTSGs, Fig. 6 (b) and Fig. 6 (c), since reversing the field winding voltage drives the field current to the rated current value. The effect of the field winding control is minor for the iron cored HTSG, Fig. 6 (a), since regardless of the control strategy, the peak field winding current under SCC is, at least, 17% higher than the rated value.

It is worth noting that the results agree with the ones presented in [16] where it is stated that the field winding current is influenced only by a few percent due to the field winding control strategy.

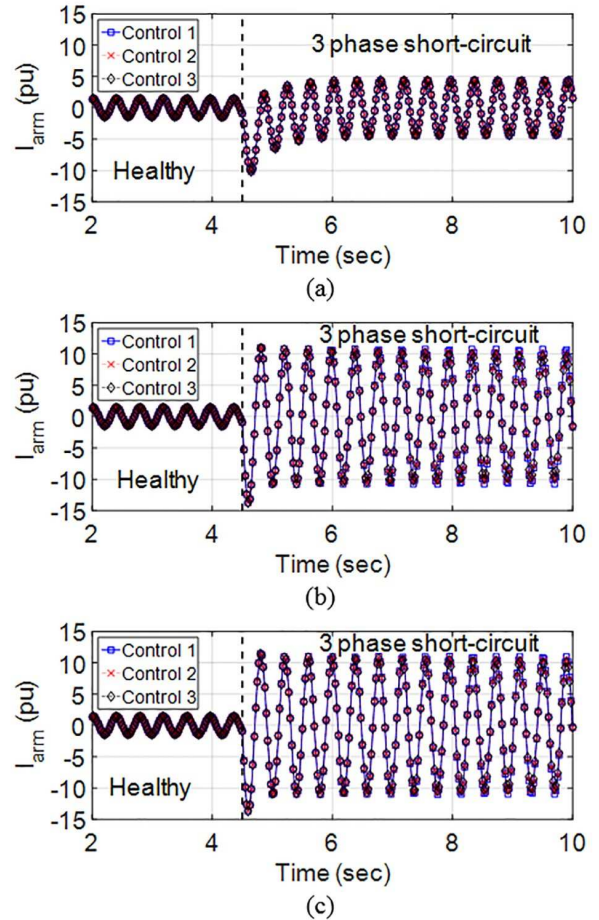


Fig. 7 Armature current variation when three phase short circuit occurs. (a) Iron cored, (b) Mixed cored, and (c) Air cored HTSG.

TABLE II EFFECT OF THE CONTROL STRATEGY ON THE PEAK ARMATURE AND PEAK FIELD WINDING CURRENTS

| HTSG | Control strategy | Peak field current (pu) | Peak armature current (pu) |
|-------------|------------------|-------------------------|----------------------------|
| Iron Cored | 1 | 1.488 | 10.152 |
| | 2 | 1.485 | 10.152 |
| | 3 | 1.481 | 10.151 |
| Mixed Cored | 1 | 1.203 | 13.766 |
| | 2 | 1.194 | 13.762 |
| | 3 | 1.187 | 13.757 |
| Air Cored | 1 | 1.197 | 13.632 |
| | 2 | 1.183 | 13.629 |
| | 3 | 1.174 | 13.626 |

IV. INFLUENCE OF OPERATING FIELD CURRENT ON PEAK ARMATURE AND PEAK FIELD CURRENTS UNDER SCC

In the previous section it is shown that the field winding control slightly influences the peak armature and peak field currents. The worst scenario is when the field winding control keeps the field winding voltage constant at its rated value. In this section the influence of the operating field current on the peak armature and peak field currents under SCC is studied when the voltage at the field winding is kept constant at the rated value.

The study is carried out by simulating a three-phase short-circuit at the HTSG terminals. For each studied HTSG, three different operating field winding currents (0.25, 0.5 and 1 pu) have been considered.

A. Influence on Peak Armature Current

The variation of peak armature current for each topology is plotted against the operating field current in Fig. 8. It shows that the peak armature current is much higher (~14 times their pu value) for the mixed and air cored HTSG than that for the iron cored HTSG in which peak armature current is only around 10 times its pu value.

These high values of the armature current under SCC are due to low values of the synchronous, transient and subtransient reactances of HTSG. Fig. 8 shows that the variations of the three peak armature currents for each HTSG are linear with the operating field current. Furthermore, it can be concluded that the mechanical supports for the structure of the mixed and air cored HTSGs need to be stronger than that for the iron cored HTSG since the peak armature current is higher, so does the transmitted magnetic force. Hence, this has to be taken into consideration at the design stage of the mechanical support.

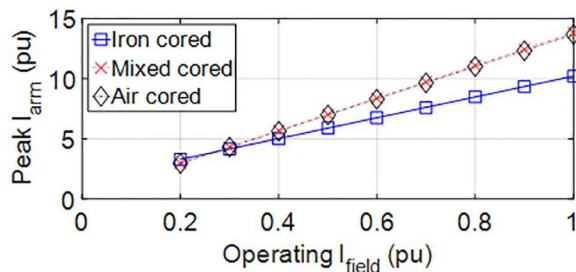


Fig. 8 Operating field current vs peak armature current.

B. Influence on Peak Field Current

A similar analysis to that carried out in the subsection IV.A is done for the peak field current in this subsection.

The influence on the peak field current is also linear with the operating field current as shown in Fig. 9. The linearity of the peak field current versus the operating field current, although simulated for high power HTSGs (10 MW), agree with the experimental results reported in [4] and [18] where a mixed cored HTSG and an iron cored HTSG of 100 kW are tested under three-phase SCC. Results show that the increase in the field current is higher for the iron cored HTSG than for the mixed and air cored HTSGs, Fig. 9. The importance of these results is that they allow designers to determine the amount of extra superconducting material needed in the field winding to avoid quench under a three-phase short circuit fault.

According to Fig. 9, at rated condition and under a three-phase short circuit the superconducting field winding should endure an extra 50% current to keep in the superconducting region for the iron cored HTSG, whereas for a mixed or air cored HTSG the superconducting winding only has to endure a 15% overcurrent.

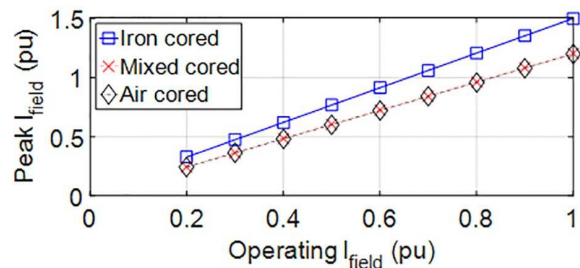


Fig. 9 Operating field current vs peak field current.

V. INFLUENCE OF THE SHORT-CIRCUIT CLEARING TIME ON PEAK ARMATURE AND FIELD CURRENTS

Circuit breakers are one of the most common devices to protect electric power systems. The time that a circuit breaker needs to clear a fault influences the peak value of the armature and field currents which a HTSG has to endure.

In the previous sections the increase of the peak armature and peak field currents when a three-phase short circuit occurs without the influence of circuit breakers has been discussed. Price of HTS superconducting materials is currently high. Therefore, it might be preferred to disconnect the HTSG from the power system rather than to add extra superconducting material to guarantee that the field winding keeps operating in the superconducting region. This can be achieved by employing circuit breakers. However, disconnecting the machine from the power system would not prevent the peak armature and peak field currents from occurring. The peak armature and peak field currents will depend on how long the chosen circuit breakers need to be disconnected from the power system after the fault.

This section deals with this problem. To study the effect of circuit breakers on the peak armature and peak field currents, two commercial circuit breakers are chosen. The first breaker is manufactured by Eaton and it is able to clear a short circuit in 36 ms [21]. The second breaker is manufactured by ABB and it is able to clear a short circuit in 80 ms [22]. The study of the influence of clearing time on the peak currents is carried out through three simulations for each studied HTSG. In each simulation the HTSG is working at the rated conditions before short-circuit occurs at 4.5 seconds. Then, for the first simulation a clearing time equal to 36 ms (Eaton circuit breaker) is set. The second simulation sets a clearing time equal to 80 ms (ABB circuit breaker). For comparison, a third simulation with a much longer clearing time equal to 1.17 seconds, three electrical cycles of the HTSG is done.

A. Influence on Armature Current

The variations of the armature current when a three-phase short circuit happens for Iron, Mixed and Air cored HTSGs, respectively, are shown in Fig. 10 for three

different clearing times. The blue squares represents the three-phase short circuit current variation for a fault cleared in 1.17 sec. However, the red crosses and black diamonds represent the fault clearing time of 80 ms and 36 ms, respectively.

TABLE III INFLUENCE OF CIRCUIT BREAKERS ON THE PEAK ARMATURE CURRENT

| HTSG | ΔT_c (sec) | Peak armature current value (pu) | Time of peak armature current (sec) | ΔT_p (sec) |
|-------------|--------------------|----------------------------------|-------------------------------------|--------------------|
| Iron Cored | 0.036 | 8.675 | 4.622 | 0.122 |
| | 0.080 | 8.675 | 4.622 | 0.122 |
| | 1.170 | 10.153 | 4.648 | 0.148 |
| Mixed Cored | 0.036 | 11.058 | 4.583 | 0.083 |
| | 0.080 | 13.766 | 4.605 | 0.105 |
| | 1.170 | 13.766 | 4.605 | 0.105 |
| Air Cored | 0.036 | 11.364 | 4.573 | 0.073 |
| | 0.080 | 13.632 | 4.600 | 0.100 |
| | 1.170 | 13.632 | 4.600 | 0.100 |

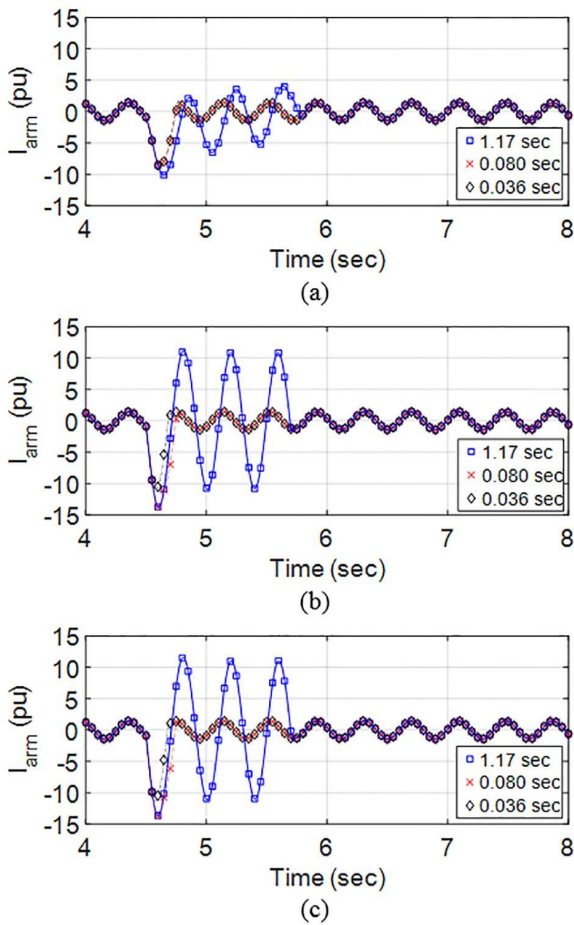


Fig. 10 Armature current variation. (a) Iron cored, (b) Mixed cored, and (c) Air cored HTSG.

Table III shows the numerical results of simulations, where ΔT_c is the fault clearing time while ΔT_p is the time for armature current to reach its peak value. The numerical results show that for an iron cored HTSG both circuit breakers reduce the peak armature current by around 15%, from 10.153 to 8.675 pu. Therefore, there is no influence on the peak armature current when the clearing time of the circuit breaker is equal or less than 80 ms, Fig. 10 (a). If the short circuit is cleared in three electrical cycles, 1.17 seconds, there is no reduction in the peak armature current

compared to the peak armature current for a permanent short-circuit, Table II.

In the case of mixed and air cored HTSGs, the results show that only the fastest circuit breaker (36 ms), is able to reduce the peak armature current by 19.66%, from 13.766 to 11.058 pu, and by 16.64%, from 13.632 to 11.364 pu, respectively. Whereas if the short-circuit is cleared in 80 ms or more, there is no reduction in the peak armature current, as confirmed in Fig. 10 (b), Fig. 10 (c) and in Table III.

B. Influence on Field Current

The use of circuit breakers to clear the fault also has influence on the value of the peak field current.

As in the previous subsection, the same cases are studied but now from the peak field current point of view. The variation of the field current under a three-phase short circuit fault is shown in Fig. 11 for the three HTSG. Table IV summarizes the increase of the peak field current as a function of the fault clearing time for each HTSG. The results show that the use of circuit breakers for the iron cored HTSG is able to reduce the peak field winding current by around 13.58% from 1.488 to 1.286 pu, i.e. regardless the circuit breaker chosen.

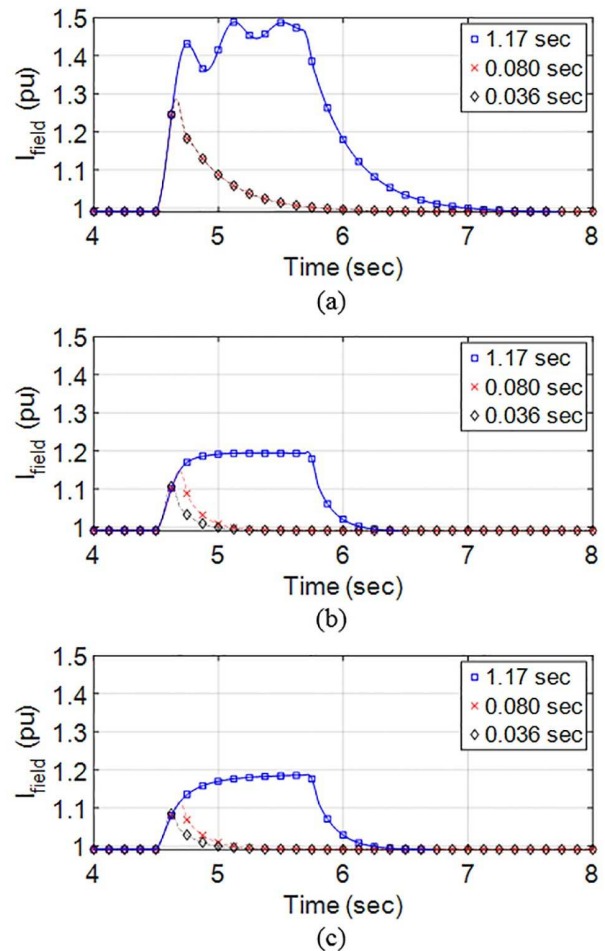


Fig. 11 Field current variation. (a) Iron cored, (b) Mixed cored and (c) Air cored HTSG.

For the mixed and air cored HTSGs, the reductions in the peak field current are much smaller than that for the iron cored counterpart, it is about 3.98%, from 1.206 to 1.158 pu, and 6.02%, from 1.196 to 1.124 pu, respectively,

for the slowest circuit breaker with a clearing time of 80 ms. The reduction of the peak field current can be increased by using the fastest circuit breaker with a clearing time of 36 ms, up to 7.55% reduction, from 1.206 to 1.115 pu, and an 8.61% reduction, from 1.196 to 1.093 pu, respectively. Unlike in the previous subsection, the use of circuit breakers reduces more significantly the peak current for the iron cored HTSG than that for the mixed or air cored HTSG.

TABLE IV INFLUENCE OF CIRCUIT BREAKERS ON PEAK FIELD CURRENT

| HTSG | ΔT_c (sec) | Peak field current (pu) | Time of peak field current (sec) | ΔT_p (sec) |
|-------------|--------------------|-------------------------|----------------------------------|--------------------|
| Iron Cored | 0.036 | 1.286 | 4.661 | 0.161 |
| | 0.080 | 1.286 | 4.661 | 0.161 |
| | 1.170 | 1.488 | 5.125 | 0.625 |
| Mixed Cored | 0.036 | 1.115 | 4.623 | 0.123 |
| | 0.080 | 1.158 | 4.685 | 0.185 |
| | 1.170 | 1.206 | 5.670 | 1.170 |
| Air Cored | 0.036 | 1.093 | 4.622 | 0.122 |
| | 0.080 | 1.124 | 4.683 | 0.183 |
| | 1.170 | 1.196 | 5.670 | 1.170 |

VI. CONCLUSIONS

This paper has made a comparative study of the influence of the field winding control on the peak armature and peak field winding currents for three 10 MW HTSGs (Iron, Mixed and Air cored). It is concluded that the field winding control has no influence on the peak currents for iron cored HTSG, and a very little influence (~1.5% reduction of the peak currents) on the mixed and air cored HTSGs. Regarding the fault ride capabilities it has been shown that a more complicated control field strategy together with a reversible field converter (control strategy 3) is unable to provide the iron cored HTSG with the necessary fault ride capability. However, for mixed and air cored HTSG such strategy is able to reduce the field winding current to acceptable levels. The main drawback of the control strategy 3, compared to the other two strategies, is the cost.

Secondly, the influence of the operating field current on the peak armature and field current has been studied. Results show that the variations of both peak currents are linear with the operating field current. Furthermore, the values of the peak armature current are higher for the mixed and air cored HTSGs than that for the iron cored HTSG. The peak field current is also linear with the operating field current but in this case the increase in the field current is higher for the iron cored HTSG than those for the mixed and air cored counterparts. Although the results are obtained by the simulations of high power HTSGs, they still agree with the previous laboratory findings for smaller power HTSGs. The influence of the operating field current on the peak field current also allows designers to determine the amount of extra superconducting material needed in the field winding to avoid quench under SCC.

Finally, the influence of the clearing time is analyzed for two different circuit breakers. It has been shown that for the iron cored HTSG the peak armature current can be reduced by 15%. Whereas, for the mixed and air cored

HTSG, the reductions in peak armature current are 19.66% and 16.64%, respectively. Regarding the peak field current, the reduction for the iron HTSG is 13.58% and smaller for the mixed (8.61%) and air (7.55%) cored HTSG for the best scenario. Furthermore, the iron cored HTSGs are less restrictive with the clearing time, since circuit breakers with 80 ms of clearing time can achieve the same results as the circuit breakers with 36 ms clearing time. However, for the mixed and air cored HTSGs, the results have shown that the smaller the clearing time, the better.

VII. REFERENCES

- [1] A.B. Abrahamsen, N. Magnusson, B.B. Jensen, and M. Runde, "Large superconducting wind turbine generators," *Energy Procedia*, vol. 24, pp.60-67, 2012.
- [2] S.S. Kalsi, "Superconducting wind turbine generator employing mgb_2 windings both on rotor and stator," *IEEE Trans. Appl. Supercond.*, vol.24, no.1, pp.47-53, Feb. 2014.
- [3] Y. Xu, N. Maki, and M. Izumi, "Performance comparison of 10 MW wind turbine generators with HTS, copper, and PM excitation," *IEEE Trans. Appl. Supercond.*, vol.25, no.6, pp.1-6, Dec. 2015
- [4] W.O.S. Bailey, Y. Yang, C. Beduz, and K.F. Goddard, "Short circuit tests on a coreless HTS synchronous generator," *IEEE Trans. Appl. Supercond.*, vol.23, no.3, pp.5201505-5201505, June 2013
- [5] H. Hatta, T. Nitta, S. Muroya, Y. Shirai, and T. Kitagawa, "Experimental study on sudden-short-circuit characteristic of synchronous generator with SCFCL," *IEEE Trans. Appl. Supercond.*, vol.11, no.1, pp.2343-2346, Mar 2001
- [6] S. Kalsi, "Applications of high temperature superconductors to electric power equipment," IEEE Press, Wiley, 2011
- [7] N. Maki, "Design study of high-temperature superconducting generators for wind power systems," *Journal of Physics: Conference Series*, 97:012155, February 2008.
- [8] G. Snitchler, B. Gamble, C. King, and P. Winn, "10 MW Class superconductor wind turbine generators," *IEEE Trans. Appl. Supercond.*, vol.21, no.3, pp.1089-1092, June 2011
- [9] T. Terao, M. Sekino, and H. Ohsaki, "Electromagnetic design of 10 MW class fully superconducting wind turbine generators" *IEEE Trans. Appl. Supercond.*, vol.22, no.3, pp.5201904-5201904, June 2012
- [10] N. Kim, G. Kim, K. Kim, M. Park, I. Yu, S. Lee; E. Song and T. Kim, "Comparative analysis of 10 MW class geared and gearless type superconducting synchronous generators for a wind power generation system," *IEEE Trans. Appl. Supercond.*, vol.22, no.3, pp.5202004-5202004, June 2012
- [11] H. Sung, G. Kim, K. Kim, S. Jung, and M. Park, "Practical design of a 10 MW class superconducting wind power generator considering weight issue," *IEEE Trans. Appl. Supercond.*, vol. 23, no. 23, pp. 5201805,2501805, June 2013
- [12] H. Sung, G. Kim, K. Kim, M. Park, I. Yu, and J. Kim, "Design and comparative analysis of 10 MW class superconducting wind power generators according to different types of superconducting wires," *Physica C: Superconductivity*, Volume 494, pp. 255-261, November 2013
- [13] Y. Xu, N. Maki, and M. Izumi, "Electrical design study of 10-MW salient-pole wind turbine HTS synchronous generators," *IEEE Trans. Appl. Supercond.*, vol.24, no.6, pp.1-6, Dec. 2014
- [14] H. Karmaker, M. Ho, and D. Kulkarni, "Comparison between different design topologies for multi-megawatt direct drive wind generators using improved second generation high temperature superconductors," *IEEE Trans. Appl. Supercond.*, vol.25, no.3, pp.1-5, June 2015
- [15] X. Song, N. Mijatovic, B.B. Jensen, and J. Holboll, "Design study of fully superconducting wind turbine generators," *IEEE Trans. Appl. Supercond.*, vol.25, no.3, pp.1-5, June 2015
- [16] K. Sivasubramaniam, X. Huang, E.T. Laskaris, T. Zhang, J.W. Bray, J.M. Forgarty, and R.A. Nold, "Performance of an HTS

- generator field coil under system fault conditions," *IEEE Trans. Appl. Supercond.*, vol.16, no.4, pp.1971-1975, Dec. 2006
- [17] S. Jung, G. Kim, H. Sung, K. Kim, M. Park, I. Yu, K.L. Kim, H. Lee, and A. Kim, "Stator winding fault influence on the field coil of a 10 MW superconducting synchronous generator," *IEEE Trans. Appl. Supercond.*, vol.23, no.3, pp.5200104-5200104, June 2013
- [18] H. Wen; W. Bailey, M.K. Al-Mosawi, K. Goddard, C. Beduz, and Y. Yang, "Further testing of an "iron-cored" HTS synchronous generator cooled by liquid air," *IEEE Trans. Appl. Supercond.*, vol.21, no.3, pp.1163-1166, June 2011
- [19] J. Pyrhonen, T. Jokinen, and V. Hrabovcova, "Design of rotating electrical machines", 1st ed., Wiley, 2009.
- [20] P.C. Krause,"Analysis of electric machinery", McGraw-Hill, 1986
- [21] Eaton. (2013, March). *38 kV Type VCP-Wind medium voltage vacuum circuit breakers, structures, and accessories* [Online]. Available:<http://www.eaton.com/ecm/groups/public/@pub/@electrical/documents/content/pl01301020e.pdf>
- [22] ABB (2014, January 27). *ANSI indoor vacuum circuit breaker ADVAC* [Online]. Available: <http://new.abb.com/medium-voltage/apparatus/circuit-breakers/indoor-CB/ansi-indoor-vacuum-circuit-breaker-advac>